Journal of Alloys and Compounds 489 (2010) 362–368

Contents lists available at ScienceDirect

Journal of Alloys and Compounds

journal homepage: www.elsevier.com/locate/jallcom

Experimental investigation on the phase equilibria of the Mn–Ni–Zn system at 400 °C

Jian lie Liang[a,b,c], Yong Du[a,*], Chang zhong Liao[b,c], Yi yuan Tang[b], Liang qin Nong[b], Feng Zheng[d], Hong hui Xu[a]

[a] State Key Laboratory of Powder Metallurgy, Central South University, Changsha Hunan 410083, PR China
[b] Institute of Materials Science, Guangxi University for Nationalities, Nanning Guangxi 530006, PR China
[c] Key Laboratory of Nonferrous Metals and New Processing Technology of Materials, Ministry of Education (Guangxi University), Nanning Guangxi 530004, PR China
[d] School of Materials Science and Engineering, Central South University, Changsha, Hunan, 410083, PR China

ARTICLE INFO

Article history:
Received 28 July 2009
Received in revised form 11 August 2009
Accepted 13 August 2009
Available online 24 August 2009

Keywords:
Phase equilibria
Mn–Ni–Zn
X-ray diffraction
Scan electron microscope

ABSTRACT

Partial isothermal section of the Mn–Ni–Zn system at 400 °C was experimentally established by means of XRD and SEM/EDS techniques. Three ternary compounds, i.e. T, τ_1 and τ_2, were found to exist at 400 °C for the first time. The compound T having an approximate formula of $Mn_7Ni_7Zn_{86}$ was indexed as fcc structure with a lattice parameter of $a = 1.81476\ (1)$ nm. τ_1, the structure of which is unknown, has an approximately stoichiometric composition of about 29 at.% Mn, 38 at.% Ni and balanced Zn. τ_2 has fcc structure and a composition range of about 46–40 at.% Mn and constant 30 at.% Zn. Extended single-phase regions of the phases Mn_5Zn_{21}, Ni_2Zn_{11}, $NiZn_3$, NiZn and β-Mn were observed. The maximum solubility of Ni in Mn_5Zn_{21} and those of Mn in Ni_2Zn_{11}, $NiZn_3$ and NiZn were determined to be 10, 6, 26 and 25 at.% at 400 °C, respectively.

1. Introduction

Zn is widely used as the protective coatings of the steel parts and components through the hot-dip galvanizing process. Mn and Si are the common alloying elements of high-strength steels. The addition of Al and Ni in the molten Zn bath was reported to be able to suppress the Sandelin effect [1] related to the Si bearing steel. Therefore, knowledge of the interaction of the alloying elements with the liquid Zn and Fe is quite important for the galvanizing industry. It was reported that information on the Al–Fe–Zn system had been effectively applied to the galvanizing industry for the determination of effective Al content in the molten bath, the management of the dross generation and the prediction of the Al consumption [2]. Several galvanizing-related alloy systems, such as Fe–Ni–Zn [3], Fe–Sn–Zn [4], Fe–Ti–Zn [5], Al–Fe–Zn [6], Fe–Mn–Zn [7], Cr–Fe–Zn [8], Bi–Ni–Zn [9] and Al–Mo–Zn [10], were experimentally investigated. In addition, the phase equilibria in some quaternary systems, such as Zn–Fe–Ni–Ti [11] and Zn–Fe–Ni–Si [12], were also experimentally studied. So far, however, no information on the phase equilibria in the Mn–Ni–Zn ternary system is available in the literature. The objective of the present work is to determine the isothermal section of the Mn–Ni–Zn system at 400 °C.

Hansen [13] early summarized the work on the phase diagram of the Mn–Zn binary system. Later, Okamoto and Tanner performed a review on this system [14]. They proposed that the ε phase ($MnZn_3$) could be divided into three phase regions (ε, ε_1 and ε_2), mainly based on the work of Wachtel and Tsiuplakis [15]. However, later and former experimental investigations on this system [16–20] showed no indication of phase separation. Recently, our research group confirmed the phase separation of the ε phase by means of a diffusion couple technique [21]. However, no convincing result from X-ray diffraction (XRD) is presented to support this viewpoint up to now.

Regarding the Ni–Zn phase diagram, Nash and Pan [22] summarized the work on this system. According to the phase diagram assessed by Nash and Pan [22], four intermediate compounds, viz. tetragonal-NiZn, cubic-NiZn, Ni_2Zn_{11} (γ) and Ni_3Zn_{22} (δ), existed in this system. The Ni_2Zn_{11} phase was reported to crystallize in space group of $I\bar{4}3m$ in composition range from 15.9 to 19.7 at.% Ni [23], while Ni_3Zn_{22} existed in space group of $C\,2/m$ in a narrow composition range [24]. It is worthy noting that Ni_2Zn_{11} and Ni_3Zn_{22} were cited as Ni_3Zn_{14} and $NiZn_8$ in the Pearson Handbook [25]. $NiZn_3$ (γ_1), which was regarded as an independent phase in the former work [26], was treated as an identical phase to Ni_2Zn_{11} in ref.22, according to the suggestion of Morton [27,28]. This result

* Corresponding author. Tel.: +86 731 88836213; fax: +86 731 88710855.
E-mail address: yonyduyong@gmail.com (Y. Du).

0925-8388/$ – see front matter © 2009 Published by Elsevier B.V.
doi:10.1016/j.jallcom.2009.08.081

was accepted in the later thermodynamic assessments of the Ni–Zn system [29–31]. The crystal structure of $NiZn_3$ (γ_1) was determined to be orthorhombic by Nover and Schubert [32] using the single crystal method. Bhan et al. [33] reviewed the experimental investigations on the Mg–Ni–Zn related systems and claimed that $NiZn_3$ exist in a triclinic structure. By using a Ni–Zn reaction diffusion couple, Dybkov and Duchenko [34] observed two sub-layers in the γ-layer (composition range from 73.1 to 86.2 Zn at.%). Nevertheless, their XRD results showed the existence of $NiZn_3$ rather than Ni_2Zn_{11}. Recently, Chumak et al. [35–36] investigated the phase equilibria of the Ni–Zn–Ge and Ni–Zn–Sb systems at 297 °C, and reported that the $NiZn_3$ phase was not observed. Thus, it is also our concern to ascertain whether the $NiZn_3$ phase stably exists at 400 °C.

Recently, Guo and Du [37] reviewed the Mn–Ni system and thermodynamically assessed the phase diagram. According to the results of ref.37, there are three intermetallic compounds, viz. α-MnNi, $MnNi_2$ and $MnNi_3$, in this binary system at 400 °C.

2. Experimental procedures

Pure elements Mn (99.9%) and Zn (99.9%) and Ni (99.95%) were used as starting materials. Forty-seven alloys were prepared by the following process. The accurately weighed ingredients were sealed in evacuated quartz tubes, and then heated up to a temperature sufficiently above the liquidus. To improve the homogeneity of the molten alloys, the quartz tubes were shaken and inversed several times, followed by furnace cooling to room temperature. Most alloys were annealed at 400 °C for 30 days. Selected alloys were further annealed for additional 50 days to ensure equilibrium state. In order to clarify the stability of the Mn_5Zn_{21} phase, selected alloys close to Mn_5Zn_{21} were held at 350 °C for 5 days. After annealing, the samples were quenched into cold water without breaking the tubes.

Each of the equilibrated alloys was cut into two parts, one for XRD analysis and another for scanning electron microscopy (SEM). The specimens were grinded into powder for XRD. It was found that alloys with high Mn contents showed good ductility, and thus great inner stress was introduced to their powder samples. To release the inner stress introduced by grinding, those powder samples were re-sealed in vacuum tubes and subjected to annealing and quenching again. XRD examinations were performed on the Rikagu-2500 and XD-3 diffractometers (Purkinje General Instrument Co. Ltd.) with Cu Kα radiation by using voltage of 40 kV and current of 200 and 30 mA, respectively. Cell parameters are calculated by using program Fullprof [38]. Microstructures of the alloys were checked by both the optical microscope and SEM. Dilute nitric acid solution was used to reveal the microstructures. Chemical compositions of the alloys were analyzed on the SEM (S-3400N from HITACHI) equipped with energy dispersive X-ray spectroscopy (EDS).

3. Experimental results

Table 1 summarizes the experimental results from the XRD and SEM/EDS examinations. The phase identification of the alloys was carried out mainly based on the results of the XRD and SEM/EDS. Fig. 1 is the isothermal section of the Mn–Ni–Zn ternary system at 400 °C, which is constructed based on the present results and the information available from the accepted boundary binary phase diagrams in the literature. On this isothermal section, three new ternary compounds, denoted as T, τ_1 and τ_2, were found and identified. The XRD patterns and microstructures of representative alloys are shown in Figs. 2–3, mainly as the evidences to support the proposed three-phase equilibria.

Fig. 4 is the XRD pattern of alloy $Mn_6Ni_8Zn_{86}$, which was prepared to obtain the single T phase, revealing that this alloy consists of almost the single T phase plus trace amount of Ni_3Zn_{22}. The existence of this new ternary compound was substantiated by the XRD results for alloys 6, 7, 13 and 29–31. The EDS analysis on these alloys indicated that the T phase is approximately stoichiometric and has an average composition of $Mn_7Ni_7Zn_{86}$. The T phase was indexed to be fcc structure with cell parameter of $a = 1.81476$ (1) nm. It should be mentioned that ternary compounds with the similar composition and XRD pattern were observed in the Fe–Ni–Zn [3,39], Fe–Ti–Zn [5] and Al–Fe–Zn [6] systems. The T phase in the Fe–Ni–Zn system, having a formula of $(FeNi)Zn_{6.5}$, was determined to belong to the space group of $F\bar{4}3m$ with a lattice parameter of $a = 1.80838$ (5) nm by using the single crystal method [40]. Considering the similarity of constituent elements between the Mn–Ni–Zn and Fe–Ni–Zn systems, $Mn_7Ni_7Zn_{86}$ was supposed to be isostructural to $(FeNi)Zn_{6.5}$. Further work to refine the crystal structure of this new ternary compound by using the Fullprof [38] is in progress.

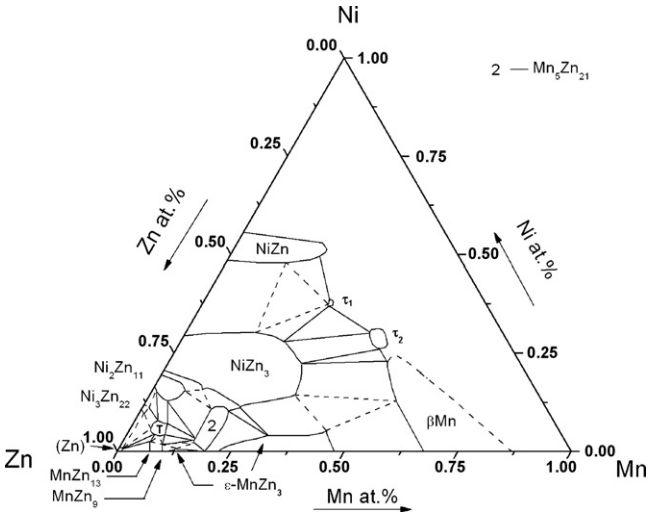

Fig. 1. Partial isothermal section of the Mn-Ni-Zn system at 400 °C.

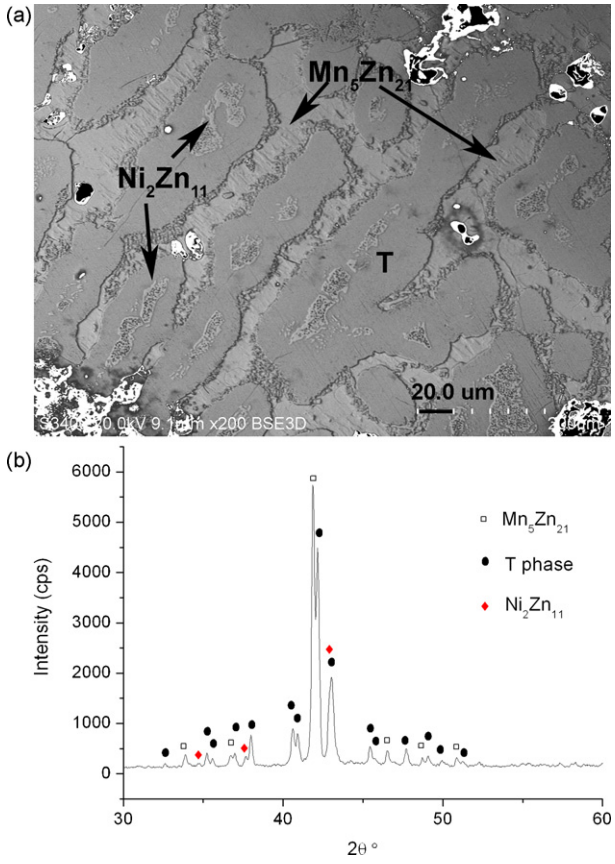

Fig. 2. (a) Microstructure of alloy 6, the deeply etched phase is Mn_5Zn_{21}, and the slightly etched phase is the T phase, while those light grey phase scattered in T phase matrix is Ni_2Zn_{11}. The white area is severely eroded region. (b) XRD pattern of alloy 6 annealed at 400 °C for 30 days, showing the co-existence of the T phase, Mn_5Zn_{21} and Ni_2Zn_{11}.

Table 1
Summary of experimental results of the Mn–Ni–Zn alloys from XRD and SEM/EDS measurements.

No.	Alloys composition (at.%)						Phases identified	Phase compositions (at.%)			Space group	Lattice parameters (nm)		
	Nominal compositions			Measured compositions				Analysis by EDS				*a*	*b*/β	*c*
	Mn	Ni	Zn	Mn	Ni	Zn		Mn	Ni	Zn				
1	35	5	60	34.2	5.9	59.9	$MnZn_3$	37.5	5.1	57.4	*P* 63/*mmc*	0.27336 (5)		0.4442 (1)
							$NiZn_3$	21.5	11.8	66.7	*Abm*2	3.381 (1)	0.9090 (3)	1.2797 (4)
2	30	5	65	27.2	7.6	65.2	$MnZn_3$	33.2	5.5	61.3	*P* 63/*mmc*	0.27395 (4)		0.44490 (9)
							Mn_5Zn_{21}	17.9	11.4	70.7	$I\bar{4}3m$	0.91142 (9)		
							$NiZn_3$	22.7	10.5	66.8	*Abm*2	3.3854 (6)	0.9082 (2)	1.2817 (2)
3	15	5	80	16.1	6.0	77.9	Ni_2Zn_{11}	Trace			$I\bar{4}3m$	0.8949		
							Mn_5Zn_{21}	16.3	6.7	77.0	$I\bar{4}3m$	0.90907 (2)		
4	20	5	75	19.8	6.0	74.2	Mn_5Zn_{21}	18.5	7.5	74.0	$I\bar{4}3m$	0.91035 (3)		
5	10	5	85	14.1	8.8	77.0	Mn_5Zn_{21}	17.4	6.7	75.9	$I\bar{4}3m$	0.90777 (7)		
							Ni_2Zn_{11}	6.5	13.7	79.8	$I\bar{4}3m$	0.89262 (4)		
6	10	5	85	8.7	6.3	85.0	Mn_5Zn_{21}	15.4	3.3	81.3	$I\bar{4}3m$	0.91311 (2)		
							Ni_2Zn_{11}	4.3	12.7	83.0	$I\bar{4}3m$	0.89357 (4)		
							T	7.0	6.9	86.1	$F\bar{4}3m$	1.81431 (1)		
7	5	5	90	5.8	8.8	85.4	Ni_2Zn_{11}	0.7	15.8	83.5	$I\bar{4}3m$	0.8912		
							T	5.7	6.9	87.4	$F\bar{4}3m$	1.81476 (1)		
8	35	10	55	39.3	9.4	51.3	$NiZn_3$	26.0	14.2	59.7	*Abm*2	3.3893 (4)	0.9059 (1)	1.2775 (2)
							$MnZn_3$	43.0	7.8	49.2	*P* 63/*mmc*	0. 27285 (3)		0.44457 (8)
9	25	10	65	23.0	11.2	65.7	$NiZn_3$	22.8	11.1	66.1	*Abm*2	3.3933 (4)	0.9056 (1)	1.2766 (2)
							$MnZn_3$	38.4	3.7	57.9	*P* 63/*mmc*	0.27366 (2)		0.44550 (7)
10	20	10	70	20.6	15.1	64.4	$NiZn_3$	17.7	18.9	63.3	*Abm*2	3.3951 (4)	0.9036 (1)	1.2739 (1)
							$MnZn_3$	25.8	7.7	66.5	*P* 63/*mmc*	0.27357 (2)		0.4445 (2)
							Mn_5Zn_{21}	19.4	10.4	70.2	$I\bar{4}3m$	0.90295 (1)		
11	15	10	75				Mn_5Zn_{21}				$I\bar{4}3m$	0.90330 (2)		
12	10	10	80	9.8	12.9	77.4	Ni_2Zn_{11}	3.8	14.6	81.6	$I\bar{4}3m$	0.89312 (6)		
							Mn_5Zn_{21}	15.3	6.1	78.6	$I\bar{4}3m$	0.91132 (5)		
13	5	10	85	6.0	9.6	84.4	Ni_2Zn_{11}	1.7	14.9	83.4	$I\bar{4}3m$	0.89284 (4)		
							T	7.6	8.0	84.4	$F\bar{4}3m$	1.81452 (2)		
14	20	15	65	20.2	16.5	63.3	$NiZn_3$	20.2	16.5	63.3	*Abm*2	3.3807 (9)	0.9008 (3)	1.2292 (4)
15	15	15	70				$NiZn_3$				*Abm*2	3.3948 (4)	0.9022 (1)	1.2739 (2)
							Ni_2Zn_{11}				$I\bar{4}3m$	0. 89828 (4)		
16	10	15	75	10.0	15.8	74.2	Ni_2Zn_{11}	9.1	17.8	73.1	$I\bar{4}3m$	0.89890 (7)		
17	5	15	80				Ni_2Zn_{11}				$I\bar{4}3m$	0.89646 (3)		
18[a]	10	35	55	10.2	38.6	51.2	NiZn	12.9	47.6	39.5	*I* 4/*mmm*	0.27392 (6)		0.32668 (7)
							$NiZn_3$	7.8	27.8	64.4	*Abm*2	3.3325 (8)	0.8899 (3)	1.2559 (4)
							NiZn	10.5	39.2	50.3	$Pm\bar{3}m$	0.2956		
19	50	10	40	35.0	14.4	50.6	β-Mn	40.0	14.1	45.9	*P*4132	0.64646 (5)		
							$NiZn_3$	32.4	15.0	52.6	*Abm*2	n.d.		

20	40	20	40	42.2	19.1	38.7	$NiZn_3$	28.9	21.0	50.1	*Abm*2	0.30179 (4)		
							β-Mn	47.3	22.4	30.3	*P*4132	0.64170 (9)		
21[b]	20	40	40	21.2	44.9	33.9	NiZn	19.0	45.3	35.7	$Pm\bar{3}m$	n.d.		
							NiZn	21.8	48.0	30.2	*I* 4/*mmm*	0.27269 (2)		0.33469 (3)
22	5	0	95				$MnZn_{13}$				*C* 2/*m*	1.34765 (3)	0.76541 (1)/β = 127.639 (1)	0.51399 (1)
							Zn				*P* 63/*mmc*	0.26647 (6)		0.49459 (8)
23	10	0	90				$MnZn_9$				Structure unknown			
24	15	0	85				$MnZn_3$				*P* 63/*mmc*	0.27629 (5)		0.44155 (5)
25	20	0	80	19.8	0	80.2	$MnZn_3$				*P* 63/*mmc*	0.27620 (2)		0.44518 (2)
26	25	0	75				$MnZn_3$				*P* 63/*mmc*	0.27536 (3)		0.44419 (3)
27	30	0	70				$MnZn_3$				*P* 63/*mmc*	0.27512 (5)		0.44540 (5)
28	40	0	60				$MnZn_3$				*P* 63/*mmc*	0.27442 (5)		0.44520 (5)
29	3	3	94				Zn				*P* 63/*mmc*	0.26644 (4)		0.49448 (4)
							T				$F\bar{4}3m$	1.81534 (1)		
							Ni_3Zn_{22}				*C* 2/*m*	n.d.		
30	3	10	87	4.2	11.1	84.7	Ni_2Zn_{11}	1.3	15.6	83.1	$I\bar{4}3m$	0.89239 (3)		
							T	6.4	6.8	86.8	$F\bar{4}3m$	1.81557 (2)		
31	8	3	89	8.7	5.1	86.2	T	7.6	5.2	87.1	$F\bar{4}3m$	1.82145 (8)		
							Mn_5Zn_{21}	10.4	6.6	83.0	$I\bar{4}3m$	Trace		
							$MnZn_9$	9.4	3.9	86.7	Structure unknown			
32	0	18	82				Ni_2Zn_{11}				$I\bar{4}3m$	0.89149 (6)		
33	0	21	79				$NiZn_3$				*Abm*2			
34	0	25	75				$NiZn_3$				*Abm*2	3.3203 (3)	0.88639 (9)	1.25105 (9)
35	0	40	60				$NiZn_3$				*Abm*2	–	–	–
							NiZn				*I* 4/*mmm*	0.2731 (4)		0.3207 (4)
36[c]	35	20	45	34.1	22.9	43.0	τ_2	46.4	24.4	29.2	–	0.37634 (1)		
							$NiZn_3$	27.7	21.4	50.9	*Abm*2			
36[d]				37.3	23.5	39.2	$NiZn_3$	30.9	22.6	46.5	*Abm*2	3.337 (6)	0.891 (1)	1.268 (3)
							τ_2	45.4	24.0	30.6	–	0.37552 (3)		
							β-Mn	49.7	23.7	26.6	*P4132*			
37[c]	30	27	43	29.5	29.7	40.8	$NiZn_3$	21.9	26.1	52.0	*Abm*2			
							τ_2	39.9	30.5	29.7	–	0.3743 (3)		
							τ_1	29.9	37.8	32.3	Structure unknown			
38[c]	35	25	40	34.6	26.1	39.3	τ_2	41.0	26.6	32.4	–	0.37479 (2)		
							$NiZn_3$	23.6	24.4	52.0	*Abm*2			
38[d]				35.4	24.5	40.1	$NiZn_3$	30.0	24.2	45.8	*Abm*2	3.336 (6)	0.8917 (9)	1.258 (2)
							τ_2	48.6	23.5	27.9	–	0.3745 (3)		
							β-Mn	47.1	24.9	28.0	*P*4132			
39	25	40	35	25.8	40.3	33.9	τ_1	27.4	38.9	33.7	Structure unknown			
							NiZn	19.8	49.3	31.0	*I* 4/*mmm*			
40[c]	30	30	40	31.0	31.9	37.1	τ_2	39.8	31.2	29.0	–			
							$NiZn_3$	21.5	29.8	48.7	*Abm*2			
							τ_1	29.6	36.5	33.9	Structure unknown			

Table 1 (*Continued*)

No.	Alloys composition (at.%)			Phases identified	Phase compositions (at.%)			Space group	Lattice parameters (nm)		
	Nominal compositions				Analysis by EDS				a	b/β	c
	Mn	Ni	Zn		Mn	Ni	Zn				
41	18	0	82	Mn_5Zn_{21}	19.0	0	81.0	$I\bar{4}3m$	0.91605 (9)		
				$MnZn_3$	18.8	0	81.2	$P\,63/mmc$	0.27615 (3)		0.44428 (6)
42	20	11	69	$NiZn_3$	21.1	11.1	67.8	$Abm2$	3.3931 (1)	0.90465 (2)	1.27677 (4)
				$MnZn_3$	26.8	10.5	62.7	$P\,63/mmc$	0.2745 (1)		0.4441 (1)
43	16	2	82	Mn_5Zn_{21}				$I\bar{4}3m$	0.91324 (4)		
				$MnZn_3$				$P\,63/mmc$	trace		
44	20	2	78	Mn_5Zn_{21}				$I\bar{4}3m$	0.91313 (3)		
				$MnZn_3$				$P\,63/mmc$	0.275		0.444
45	26	5	69	$MnZn_3$	30.9	3.3	65.8	$P\,63/mmc$	0.27426 (3)		0.4443 (1)
				Mn_5Zn_{21}	19.5	7.8	72.8	$I\bar{4}3m$	0.90718 (4)		
46	1	4	95	Zn	0.5	1.0	98.5	$P\,63/mmc$			
				T	4.7	5.4	89.9	$F\bar{4}3m$			
47	4	1	95	Zn	1.0	0.7	98.3	$P\,63/mmc$			
				T	7.8	3.1	89.1	$F\bar{4}3m$			
				$MnZn_{13}$	5.9	2.6	91.5	$C\,2/m$			

[a] The alloy was slightly off-equilibrium and trace amount of cubic-NiZn was observed by SEM.
[b] The alloy was far from equilibrium.
[c] The τ_2 phase has fcc structure with the space group unknown.
[d] The alloys were further annealed at 400 °C for additional 50 days.

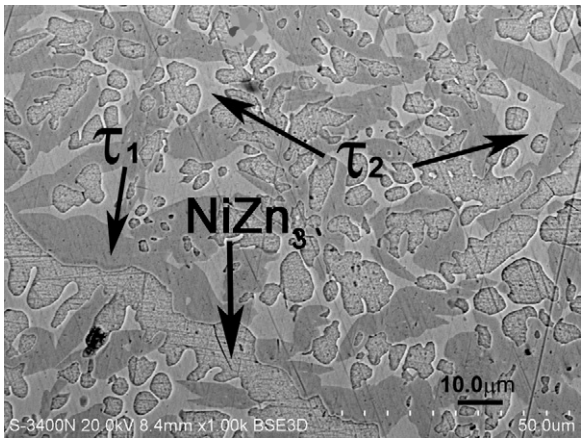

Fig. 3. Microstructure of alloy 40 annealed at 400 °C for 30 days, showing the co-existence of $NiZn_3$ and τ_1 and τ_2.

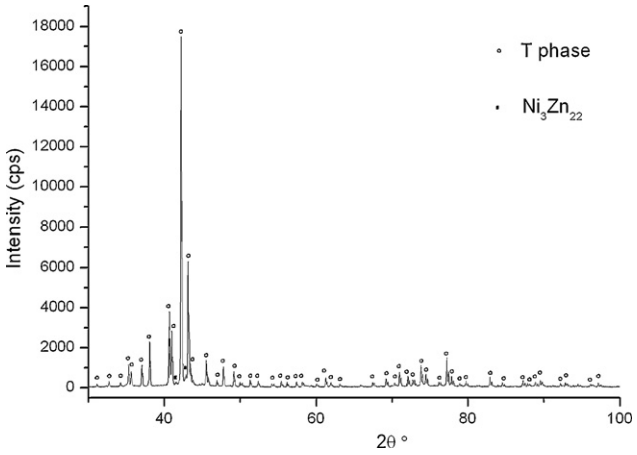

Fig. 4. XRD pattern of alloy $Mn_6Ni_8Zn_{86}$ having an overwhelming majority of the single T phase and minor amount of Ni_3Zn_{22}.

τ_1 was observed in alloys 37, 39 and 40, having close compositions to each other, i.e. $Mn_{29.9}Ni_{37.8}Zn_{32.3}$, $Mn_{27.4}Ni_{38.9}Zn_{33.7}$ and $Mn_{29.6}Ni_{36.5}Zn_{33.9}$, respectively. A formula of $Mn_7Ni_9Zn_8$ for this ternary compound was deduced. Fig. 5 presents the microstructure of alloy 39, showing the co-existence of τ_1 with minor amount of tetragonal-NiZn.

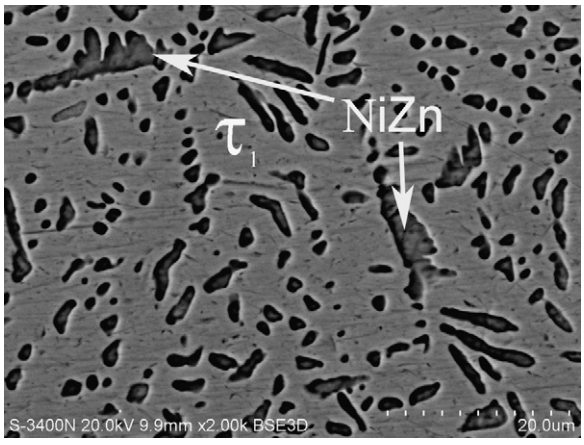

Fig. 5. Back scattered electron image of alloy 39 annealed at 400 °C for 30 days. The matrix is τ_1, and the scattered phase in matrix is tetragonal-NiZn.

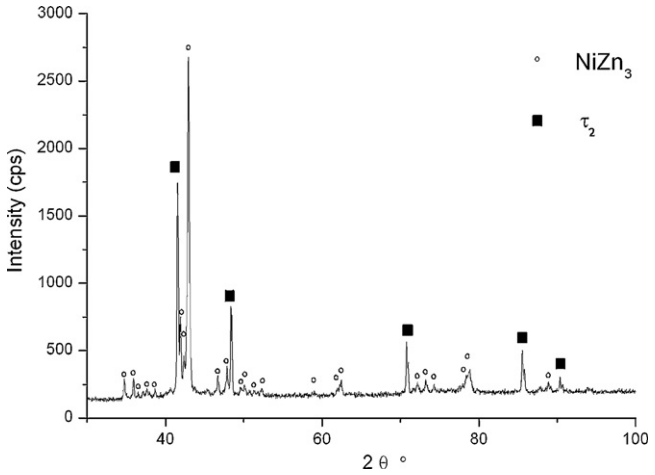

Fig. 6. XRD pattern of alloy 36 annealed at 400 °C for total 80 days, showing the co-existence of $NiZn_3$ with τ_2.

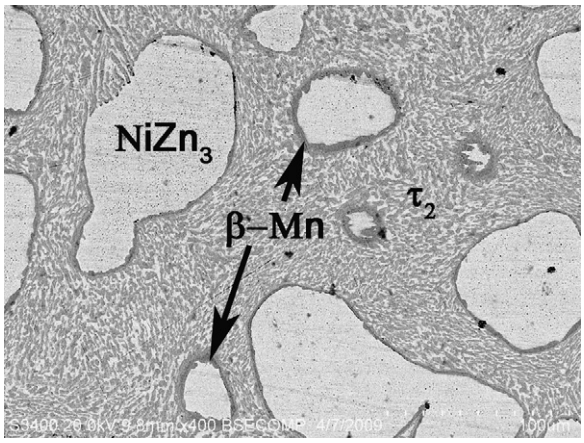

Fig. 7. Back scattered electron image of alloy 36 annealed at 400 °C for 80 days. The light grey phase (the large island and strip phases) is $NiZn_3$, and the deeply grey phase surrounding the $NiZn_3$ is β-Mn, while the grey phase eutectoidly mixed with $NiZn_3$ is τ_2.

τ_2 has a fcc structure and a composition range from about 46 to 40 Mn at.%, 24 to 30 Ni at.% and a fixed Zn content of nearly 30 at.%. Fig. 6 presents the XRD pattern of alloy 36, which is clearly characterized as the two phases τ_2 and $NiZn_3$.

Alloy 34 ($Ni_{25}Zn_{75}$) was found to consist of a single $NiZn_3$ phase. The $NiZn_3$ phase was detected in alloys 1, 2, 8–10, 14–15 and 18–20. Thus, it can be concluded that $NiZn_3$ has an extended solution region with Mn partially substituted for Zn and Ni. The maximum solubility of Mn in $NiZn_3$ was measured to be about 26 at.%.

A primitive cubic ternary phase, which is based on the high temperature cubic-NiZn and has nearly constant Zn content of 50 at.% Zn, was certainly observed for this system at 600 °C by either XRD or SEM/EDS examination [41]. In order to ascertain whether this ternary phase is stable at 400 °C, alloy 36, consisting of both the cubic-NiZn ternary phase and τ_2, and alloy 38, characterizing of τ_2 and γ-Mn at 600 °C, were re-annealed at 400 °C for 30 days. The XRD results showed the existence of τ_2 as well as a phase containing about 50 at.% Zn in both alloys. However, it is difficult to identify the second phase other than τ_2, since contradictory results were obtained for the powders before and after the inner stress release annealing. The XRD patterns for the powders of alloys 36 and 38 without stress release annealing, seem to reveal the existence of the primitive cubic phase. Nevertheless, the broadening of the diffraction lines resulting from the working stress makes this conclusion somewhat dubious. For the powders subjected to stress release annealing, XRD identified $NiZn_3$ and τ_2 for both alloys. To determine either $NiZn_3$ or NiZn is stable in the alloys, the alloys were annealed at 400 °C for additional 50 days. After annealing, the XRD results indicated the existence of the τ_2 and $NiZn_3$ both in the annealed and un-annealed powders for these alloys. Consistent results were observed with SEM/EDS analysis but the compositions of the equilibrated phases were found to slightly change, compared with those in the alloys annealed less time, as shown in Table 1. It should be mentioned, besides τ_2 and $NiZn_3$, minor amount of β-Mn was also observed in both alloys 36 and 38 after heat-treated at 400 °C for additional 50 days, as shown in Fig. 7. Therefore, we conclude that the ternary phase, which is based on the primitive cubic-NiZn and stable at 600 °C, does not exist at 400 °C.

Separated solid solutions of Mn_5Zn_{21} and Ni_2Zn_{11} were observed in this system, though both have the identical space group $I\bar{4}3m$ and same Pearson symbol of cI 52 and close lattice parameters, $a = 0.916$ and 0.8912 nm for Mn_5Zn_{21} and Ni_2Zn_{11}, respectively. This case is different to that in the Fe–Ni–Zn system, where both of Ni_2Zn_{11} and Fe_3Zn_{10} have the same space group $I\bar{4}3m$ and form a series of continuous solid solutions [3,39]. As shown in Fig. 8, alloys 4 and 11 were characterized as a single Mn_5Zn_{21} phase, while alloys 16 and 17 as a single Ni_2Zn_{11} phase. Alloy 5 is composed of both Mn_5Zn_{21} and Ni_2Zn_{11}. The XRD results were substantiated by the SEM/EDS analysis for these alloys.

Mn_5Zn_{21} was reported to congruently transform into $MnZn_3$ at 420 °C and a composition of about 20 at% Mn [14]. In the present work, Mn_5Zn_{21} and $MnZn_3$ were observed in the alloy 41 ($Mn_{18.8}Zn_{81.2}$) quenched from 400 °C. The peak intensities of the $MnZn_3$ phase decreased dramatically after the alloy was kept at 350 °C for 5 days. Fig. 9 presents the XRD pattern and microstructure of alloy 41. As listed in Table 1, the compositions of Mn_5Zn_{21} and $MnZn_3$ were measured to be 19.0 and 18.4 at.% Mn, respectively, which is very close to each other. A single $MnZn_3$ phase was detected for alloy 25 ($Mn_{19.2}Zn_{80.8}$) annealed at 400 °C. When this alloy was hold at 350 °C for 5 days, the XRD peak intensities of the Mn_5Zn_{21} phase increased sharply while $MnZn_3$ almost diminished. As a single $MnZn_3$ phase was also observed in alloy 26 ($Mn_{25}Zn_{75}$), and both Mn_5Zn_{21} and $MnZn_3$ were observed in alloys 43 ($Mn_{16}Ni_2Zn_{82}$) and 44 ($Mn_{20}Ni_2Zn_{82}$), we assumed that Mn_5Zn_{21} might exist in a narrow composition range in Mn–Zn side, and its congruent transition temperature might be very close to 400 °C.

With regard to the $MnZn_3$ phase, no strong evidences from either XRD of the binary alloys or XRD and SEM/EDS results of

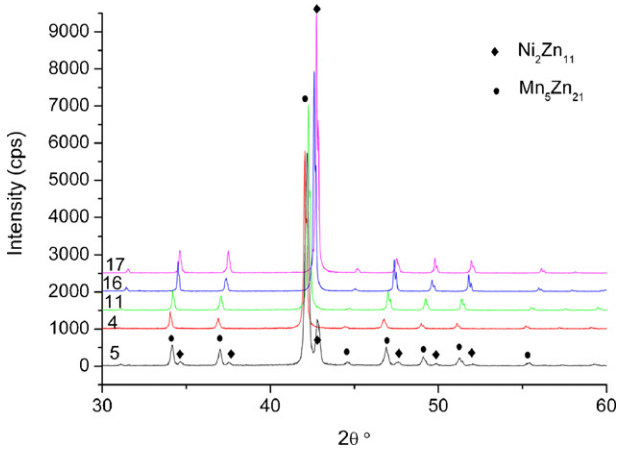

Fig. 8. XRD patterns of alloys 4, 5, 11 and 16–17 annealed at 400 °C for 30 days, showing that alloys 16 and 17 are composed of a single-phase Ni_2Zn_{11}, and alloys 4 and 11 composed of a single Mn_5Zn_{21} while alloy 5 consists of Ni_2Zn_{11} and Mn_5Zn_{21}.

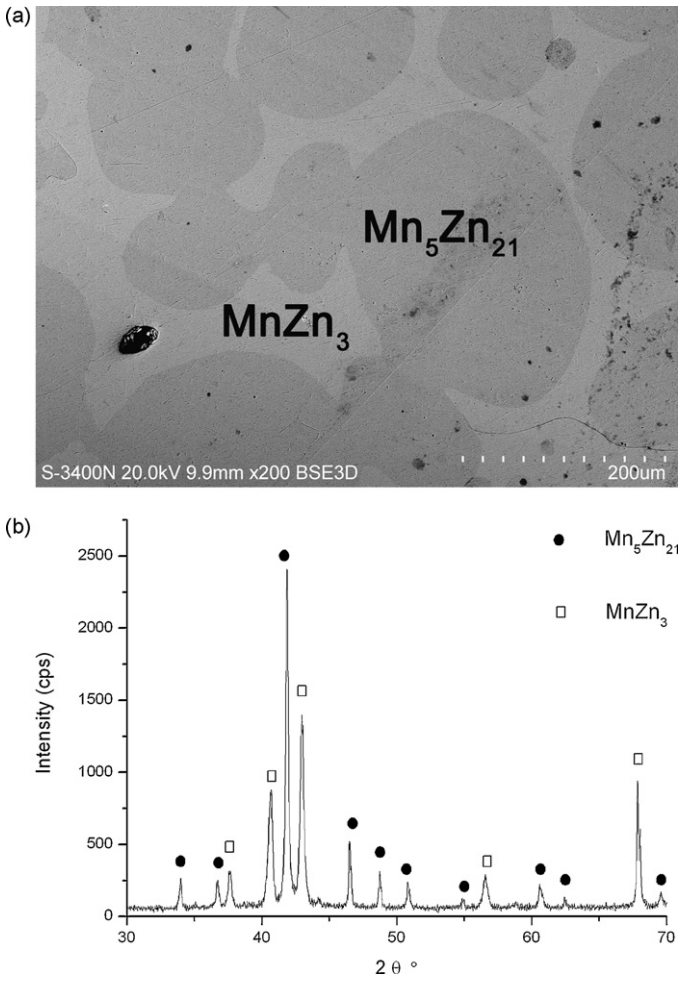

Fig. 9. (a) Microstructure of alloy 41 annealed at 400 °C for 30 days, the deeply grey phase is Mn_5Zn_{21}, and the grey phase is $MnZn_3$. (b) XRD pattern of alloy 41, showing the co-existence of Mn_5Zn_{21} with $MnZn_3$.

the ternary alloys were found to support the existence of three sub-divisions. Thus, a single $MnZn_3$ region in the Mn–Zn system is accepted in the present work.

The maximum solubility of Mn in Ni_2Zn_{11} and that of Ni in Mn_5Zn_{21} were determined to be about 6 and 10 at.%, respectively. And about 25 at.% Mn substitutes for Zn in NiZn with the Ni content nearly constant at 50 at.%.

For this isothermal section, four three-phase equilibria, i.e. (Ni_2Zn_{11} + T + Mn_5Zn_{21}), (Mn_5Zn_{21} + $NiZn_3$ + $MnZn_3$), (τ_1 + τ_2 + $NiZn_3$) and ($NiZn_3$ + τ_2 + β-Mn), are well established.

4. Conclusions

The phase equilibria in Zn-rich corner of the Mn–Ni–Zn system were investigated by means of XRD and SEM/EDS techniques. The main results are as follows:

(1) Three new ternary compounds, namely T, τ_1 and τ_2, were found and identified. The space group of the T phase is $F\bar{4}3m$ with a = 1.81476 (1) nm, and τ_2 has fcc structure.

(2) Considerable extension into the ternary system for the binary phases Mn_5Zn_{21}, Ni_2Zn_{11}, $NiZn_3$, NiZn and β-Mn was observed. The maximum solubility of Ni in Mn_5Zn_{21} and those of Mn in Ni_2Zn_{11}, $NiZn_3$ and NiZn are determined to be 10, 6, 26 and 25 at.% at 400 °C, respectively.

(3) The following four three-phase equilibria were well established: (1) (Ni_2Zn_{11} + T + Mn_5Zn_{21}), (2) (Mn_5Zn_{21} + $NiZn_3$ + $MnZn_3$), (3) (τ_1 + τ_2 + $NiZn_3$) and (4) ($NiZn_3$ + τ_2 + β-Mn).

Acknowledgements

This work is financial supported by the National Natural Science Foundation of China (Grant Nos. 50721003 and 50425103), the Guangxi Science Foundation (Contract nos. 0448022, 0540009 and 0640040), Guangxi Large Scale Apparatus Corporation Office.

References

[1] G. Reumont, P. Perrot, J. Foct, J. Mater. Sci. 33 (1998) 4759–4768.
[2] N.Y. Tang, J. Phase Equilib. Diffus. 27 (2006) 462–468.
[3] N.Y. Tang, X.P. Su, J.M. Toguri, Calphad 25 (2001) 267–277.
[4] N.Y. Tang, X.P. Su, X.B. Yu, J. Phase Equilib. Diffus. 24 (2003) 528–532.
[5] X.H. Tang, F.C. Yin, X.M. Wang, J.H. Wang, X.P. Su, N.Y. Tang, J. Phase Equilib. Diffus. 28 (2007) 355–561.
[6] N.Y. Tang, X.P. Su, Metall. Mater. Trans. A 33 (2002) 1559–1561.
[7] G. Reumont, G. Dupont, P. Perrot, Z. Metallkd. 86 (1995) 608–613.
[8] G. Reumont, M. Mathon, R. Fourmentin, P. Perrot, Z. Metallkd. 94 (2003) 411–418.
[9] Y.X. Liu, F.C. Yin, H. Tu, Z. Li, J. Wang, X.P. Su, J. Phase Equilib. Diffus. 29 (2008) 493–499.
[10] Z.H. Wang, J.H. Wang, Y.H. Liu, N.Y. Tang, X.P. Su, J. Phase Equilib. Diffus. 27 (2006) 469–476.
[11] G. Reumont, T. Gloriant, P. Perrot, J. Mater. Sci. Lett. 16 (1997) 62–65.
[12] S.W. Pan, F.C. Yin, M.X. Zhao, Y. Liu, X.P. Su, J. Alloys Compd. 470 (2009) 600–605.
[13] M. Hanson, Constitution of Binary Alloys, 2nd ed., McGraw-Hill, New York, 1958, pp. 962–963.
[14] H. Okamoto, L.E. Tanner, Bull. Alloy Phase Diagrams 11 (1990) 377–384.
[15] E. Wachtel, K. Tsiuplakis, Z. Metallkd. 58 (1967) 41–45.
[16] J. Schramm, Z. Metallkd. 32 (1940) 399–407.
[17] E.V. Potter, R.W. Huber, Trans. ASM 41 (1949) 1001–1022.
[18] W.B. Henderson, R.J.M. Willcox, Philos. Mag. 9 (1964) 829–846.
[19] O. Romer, E. Wachtel, Z. Metallkd. 62 (1971) 820–825.
[20] Y. Nakagawa, T. Hori, Trans. Jpn. Inst. Met. 13 (1972) 167–170.
[21] H.H. Xu, X. Xiong, L.J. Zhang, Y. Du, P.S. Wang, Metall. Mater. Trans. A 40 (2009) 2042–2047.
[22] P. Nash, Y.Y. Pan, Bull. Alloy Phase Diagrams 8 (1987) 422–430.
[23] A. Johansson, H. Ljung, S. Westman, Acta Chem. Scand. 22 (1968) 2743–2753.
[24] J.K. Critchley, S. Denton, J. Inst. Met. 99 (1971) 26–27.
[25] P. Villars, Pearson's Handbook: Crystallographic Data for Intermetallic Phases, Desk ed., ASM International, Materials Park, OH, 1997.
[26] J. Schramm, Z. Metallkd. 30 (1938) 122–130.
[27] A.J. Morton, Phys. Status Solidi 44 (1977) 205–214.
[28] A.J. Morton, Acta Metall. 27 (1979) 863–867.
[29] G.P. Vassilev, J. Alloys Compd. 190 (1992) 107–112.
[30] G.P. Vassilev, T. Gomez-Acebo, J.C. Tedenac, J. Phase Equilib. Diffus. 21 (2000) 287–301.
[31] X.P. Su, N.Y. Tang, J.M. Toguri, J. Phase Equilib. Diffus. 23 (2002) 140–148.
[32] G. Nover, K. Schubert, J. Less-Common Met. 75 (1980) 51–63.
[33] S. Bhan, K.C. Jain, A. Lal, J. Phase Equilib. Diffus. 18 (1997) 305–310.
[34] V.I. Dybkov, O.V. Duchenko, J. Phase Equilib. Diffus. 5 (1998) 434–440.
[35] I. Chumak, V. Pavlyuk, J. Alloys Compd. 367 (2004) 85–88.
[36] I. Chumak, V. Pavlyuk, G. Dmytriv, Intermetallics 13 (2005) 109–112.
[37] C. Guo, Z. Du, Intermetallics 13 (2005) 525–534.
[38] J. Rodríguez-Carvajal, Fullprof. http://www.ill.eu/sites/fullprof/.
[39] F. Peng, F.C. Yin, X.P. Su, L. Zhi, M.X. Zhao, J. Alloy Compd. 402 (2005) 124–129.
[40] S. Lidin, M. Jacob, A.K. Larsson, Acta Crystallogr. C 50 (1994) 340–342.
[41] J.L. Liang, Y. Du, Phase equilibria in the Mn–Ni–Zn ternary system at 600 °C, unpublished paper.